Jpn. J. Appl. Phys. Vol. 39 (2000) pp. 6619–6624
Part 1, No. 12A, December 2000

Effect of Waveform Slew-rate on Bistable Cholesteric Displays

W. C. YIP and H. S. KWOK
Department of Electrical and Electronic Engineering, The Hong Kong University of Science and Technology, Clear Water Bay, Kowloon, Hong Kong

(Received April 10, 2000; accepted for publication September 27, 2000)

Since the typical peak-to-peak voltage needed to drive the bistable cholesteric display is two to three times higher than that for super twist nematic (STN) displays, the transient current can be excessively large and detrimental to most semiconductor drivers. To reduce the maximum switching current, the voltage transition time should be restricted in addition to reducing the peak voltage. In this paper, we studied the effect of slew-rate on the maximum output current, average output power and the dynamic optical responses. Based on circuit theory, we obtained a good agreement between experimental and calculated results. The optimal settings can be incorporated into our driving scheme so that low voltage and current requirements can be met for very large-scale integration (VLSI) implementation.

KEYWORDS: bistable cholesteric display, slew-rate, transient current

1. Introduction

In the bistable cholesteric display (BCD), there are two long-lived stable states: planar and focal-conic. Since the orientation of helical axis at either state is different, the Grandjean or fingerprint texture can be observed in the respective state. To switch from the focal-conic state to the planar state, it usually requires high voltage pulses to align the liquid crystal molecules homeotropically before they are relaxed rapidly to form the planar texture. On the other hand, to switch back from the planar state to the focal-conic state, there are two possible ways. The first one is to let the liquid crystal molecules relax slowly from the field-induced homeotropic alignment. Whereas the second one is to make use of the low-voltage transition threshold beyond which the planar helical structure will be upset. The former has been proposed by the research group at the Kent State University,[1)] whilst the latter has been worked out by another group at the Hong Kong University of Science and Technology.[2)] These are the physical mechanisms for the state switching of the BCDs. Although there are recently more schemes reported, these two contributions are the most original. Currently, the addressing scheme proposed by the group at the Kent State University is the fastest, however it is very complex and composed of different stages (preparation, selection and evolution) of many switching cycles to address a pixel.[1)] Since the switching current can be excessively large during these cycles, it will cause a manifold increase in the loading and the parasitic couplings associated with these transients. To solve these problems, we have already devised an efficient driving scheme[3)] that requires only half of the drive voltage and less rapid transitions. In this paper, we shall discuss the effect of the slew-rate on the electro-optic characteristics and the optimal conditions. We shall also compare the electrical requirement between the 2 ms/line and the 4 ms/line addressing when the slew-rate is taken into account.

Although the cholesteric liquid crystal has been proposed for the display applications since the late 60 s, there is not much advancement so far to commercialize this type of display. There are still many scientific and technological issues not yet fully understood. One of the hardest problems is to understand the transition dynamics upon the application of an electric field. The permeation for example is one of the non-Newtonian flow mechanisms that has been studied since 1969. In fact, the flow properties of a cholesteric liquid crystal are surprisingly different from those of a nematic. According to de Gennes and many others, the physical flow effects and orientational effects are much more complex on a helical structure: in particular the apparent bulk viscosity of a cholesteric sample may often be 10^5 times larger than the friction coefficients defined in Leslie equations (see for example ref. 11). Therefore, the dynamics are so intrigue that the perturbation approaches break down. We model the cholesteric liquid crystal with the simple circuit elements in this paper. Consequently, the microscopic phenomena associated with the cholesteric liquid crystal will be ignored.

To compute the displacement current, the capacitance associated with the anisotropic dielectric constants is different for the different state mentioned above. Since the surface treatment and conditioning can have a profound effect on the helical axis distribution,[4,5)] we use the cells which are coated with the unrubbed polyimide in favour of the planar alignment in the following studies. The currents due to the carrier mobility and absorbed charge layers at the substrate interfaces are neglected in comparison with the displacement current.[6,7)] The circuit model for the BCD and the derived equations are described in §2, whilst the experimental results and the optimal slew-rate are discussed in §3.

2. Circuit Model

Since the resistivity of the chiral dopants is usually much larger than that of typical nematic mixtures, a simple equivalent model is described in Fig. 1(a). It consists of a bulk capacitance C_B, a bulk resistance R_B and those for the polyimide alignment layers C_P and R_P. The electrode resistance is neglected in this study. Generally, R_B is many times larger in comparison with the reactance of C_B at a typical operation frequency of 1 kHz. This ratio is equal to the product of the bulk resistivity, the bulk permitivity and the angular frequency, and does not depend on the dimensions of the liquid crystal cell. It usually varies from tens to thousands times when different liquid crystal mixtures (twist nematic, super twist nematic and active-matrix) are used. Therefore, the bulk resistance is considered insignificant compared to the bulk reactance in the following computations and this approximation will be justified in the Appendix. In Fig. 1(b), the circuit diagram for the current and power measurement is depicted. A resistor R of 1 kΩ is connected in series with the cell so

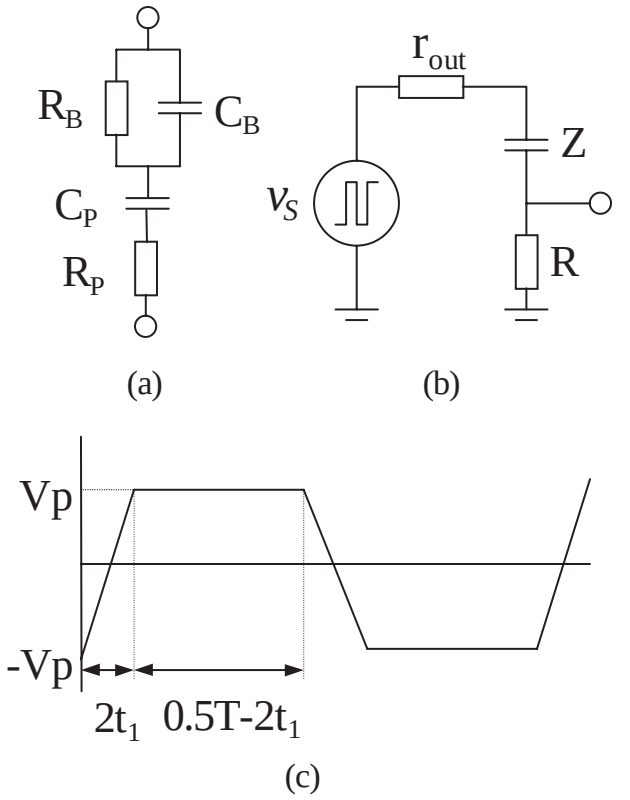

Fig. 1. (a) Equivalent circuit model of BCD used to calculate i_{max}, $\langle p_{out}\rangle$ and p_{max}. C_B and R_B are the bulk capacitance and resistance respectively, whereas C_P and R_P are those for the polyimide alignment layers. (b) Circuit diagram for the measurement of i_{max}, $\langle p_{out}\rangle$ and p_{max}. (c) Trapezoid waveform for the slew-rate control.

that the in-phase current with the source voltage v_s can be measured directly. r_{out} is the output resistance of the waveform synthesizer and the trapezoid waveform of controllable slew-rate is synthesized to study the electrical characteristics In Fig. 1(c), V_P is the peak voltage, t_1 is half of the rising edge transition time and T is the period.

Based on circuit theory, we take the approximation on the bulk resistance to derive the differential equation of the electrical charge. We further assume the full-charge condition at which the period is sufficiently long compared with the electrical time constant of the display cell. Therefore, the maximum output current, average and maximum output power during each voltage transition can be readily obtained as follows.

$$i_{max} = SC(1 - e^{-2/s}) \tag{1}$$

$$\langle p_{out}\rangle = V_P SC\left(\frac{\tau}{0.5T}\right)\{2 - s + se^{-2/s}\} \tag{2a}$$

$$p_{max} = V_P SC(1 - e^{-2/s}) \tag{2b}$$

where the slew-rate, the effective capacitance, the time-constant and the reduced slew-rate are respectively given by

$$S = \frac{V_P}{t_1} \tag{3a}$$

$$C = \frac{C_B C_P}{C_B + C_P} \tag{3b}$$

$$\tau = (R + R_P)C \tag{3c}$$

$$s = \frac{\tau}{t_1} \tag{3d}$$

Thus, i_{max} is proportional to the SC product. Whereas $\langle p_{out}\rangle$ depends on the SC product, the peak voltage and the ratio of time constant to half period, In addition, p_{max} shows a similar dependence. Reduction in the SC product will result in small switching powers and current. However, further reduction in the slew-rate S will affect the dynamic optical response. Therefore, an optimal condition exists for driving the BCD.

The change in the slew-rate will accompany a change in the root-mean-square (rms) voltage. For the constant rms the new peak voltage V_P relates the rectangular voltage amplitude V_{P0} according to

$$V_P = V_{P0}\sqrt{\frac{1 + 2x}{1 + 2x/3}} \tag{4a}$$

where the duration ratio of the rising edge to the steady state is

$$x = \frac{t_1}{0.5T - 2t_1} \tag{4b}$$

When x is equal to 1/8, less than 8% increase in peak voltage is required to keep the rms constant. In term of the slew-rate, eq. (4a) can be expressed as

$$V_P = V_{P0}\sqrt{\frac{(T/2V_{P0})S}{(T/2V_{P0})S - 4/3}} \tag{5}$$

This equation explicitly relates the voltage dependence with the slew-rate, which is central in the determination of the electrical characteristics.

To deduce the voltage increase associated with different writing times, an implicit relation is obtained below using eq. (4a).

$$\frac{y^3}{b} - \frac{3}{8}\frac{t'_w}{t_1}y^2 + \frac{3}{8}\frac{t'_w}{t_1} - 1 = 0 \tag{6}$$

where t_w and t_1 are the writing time and the half transition time of a reference case. $t_w = 4$ ms and $t_1 = 0.2$ ms are chosen so that b denotes the multiples of the slew-rate at 0.175 V/μs. The prime signifies the parameters in the increased voltage case, and the voltage ratio is

$$y = \frac{V'_P}{V_P} \tag{7}$$

In other words, eq. (6) will indicate the voltage increase when the 2 ms/line and the 4 ms/line addressing are compared at the same slew-rate for example.

3. Results and Discussions

For the measurements discussed in this section, a batch of test cells was fabricated in our laboratory. Unrubbed polyimide PIA3744 from Chisso Corp. was coated on the indium tin oxide (ITO) glass surface and nematic mixture DLC-42121 from Dainippon Ink & Chemicals Inc. was used. The cell gap was about 4 μm and the cell reflected the 543.5 nm laser light. To reduce Fresnel reflections, the electro-optic characteristics were measured in a cross-polarization setup (see ref. 3). The p-wave was reflected by the polarized beam splitter (PBS) and incident normal to the test cell. The s-wave of the circularly polarized light reflected from the cholesteric

helical structures was transmitted and detected by a silicon photo-detector. Voltage signals can be acquired and integrated real-time by a Hewlett-Packard Infinium Oscilloscope. Hence the electrical, optical and dynamic responses can be measured directly.

3.1 Electrical characteristics

The voltage across the current sensing resistor was monitored and the corresponding output currents at different slew-rate were shown in Fig. 2(a). At the slew-rate below 0.7 V/μs, the maximum current became flat and it decreased gradually on further reduction in the slew-rate. The discharging began to decay when the voltage was at the beginning of the rising edge transition. Whereas the charging happened to grow at the end of the rising edge transition. In Fig. 2(b), the maximum output current was obtained alongside the theoretical plots obtained by eq. (1). Measurements at the homeotropic and the focal-conic states were performed since the associated capacitances were different. The cell was also initialized to the planar state before the controlled waveform was applied to switch it to the homeotropic or the focal-conic state. At slow slew-rates, i_{max} was independent of resistance $R + R_P$ and the currents at the two states became comparable. At fast slew-rates, the exponential term would diminish and the current would essentially depend on the *SC* product. Hence, to operate below 1 mA/cm^2, the slew-rate should be less than 0.175 V/μs.

The product of output current and voltage was measured simultaneously and the corresponding power was shown in Fig. 3(a). The peak power occurred close to the point when the voltage reached the constant amplitude and operating at the high peak power could cause the reliability problems. When the slew-rate was reduced to 0.175 V/μs, the output power showed a more symmetrical dependence about the time axis. Consequently, the average power could be reduced to a lower value. The curves in Figs. 3(b) and 3(c) are theoretical curves calculated using eq. (2a) and eq. (2b). At the slow slew-rate, the linear dependence of average and peak power on the slew-rate was obvious and the reduction in the

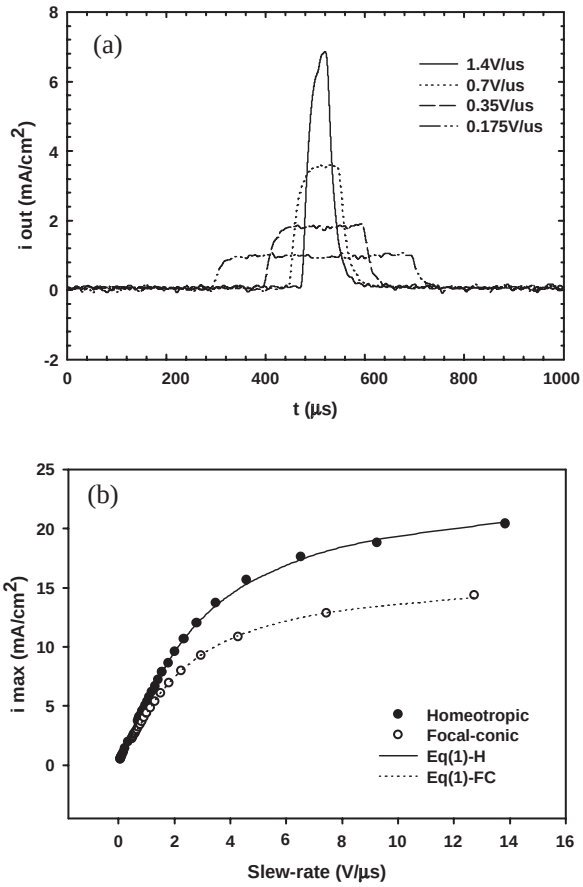

Fig. 2. (a) Output current as a function of time and (b) maximum output current against slew-rate during the rising edge transition. The frequency of the trapezoid waveform is 100 Hz.

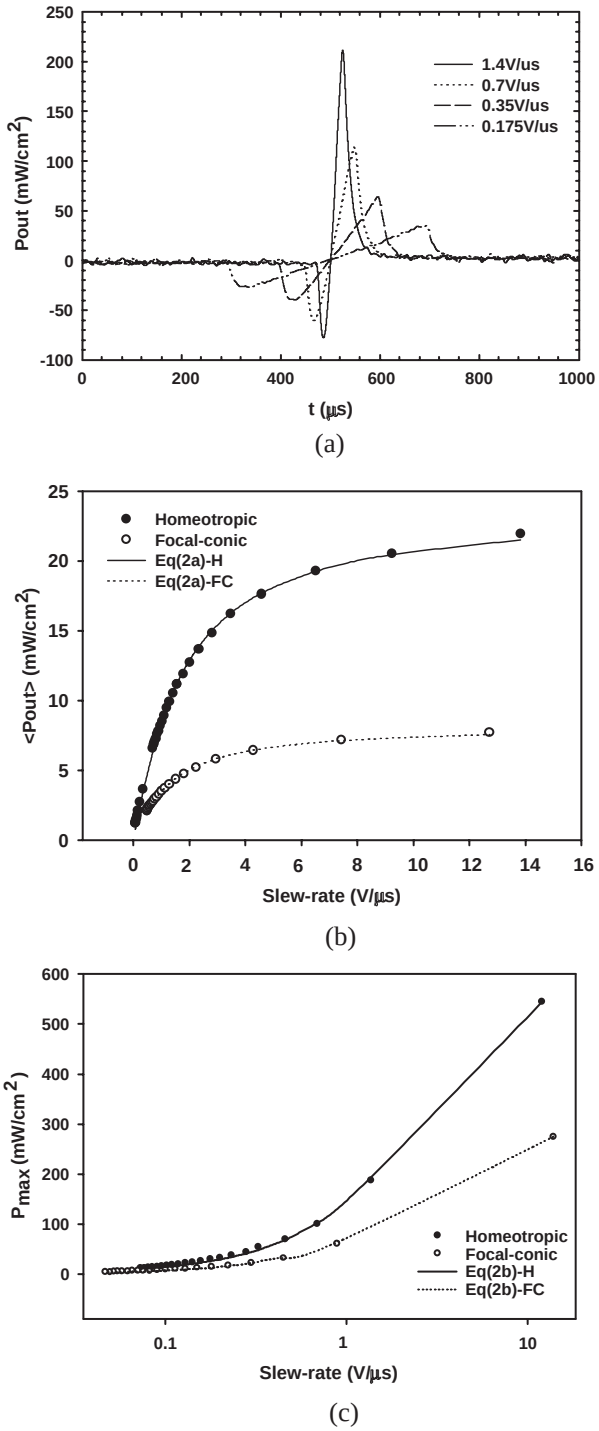

Fig. 3. (a) Output power as a function of time, (b) average and (c) maximum output power against slew-rate during the rising edge transition. The frequency of the trapezoid waveform is 100 Hz.

peak voltage in these cases could lessen the power consumption linearly. Under this trend, the average or peak power at both states also converge though the operation involved less homeotropic transitions was an advantage in general. In Fig. 2 or 3, the agreement between theory and experiment was so good that the approximation could be justified, that is, the conduction mechanism was dominated by the displacement current. All these findings will be incorporated into our driving scheme to study the dynamic optical response.

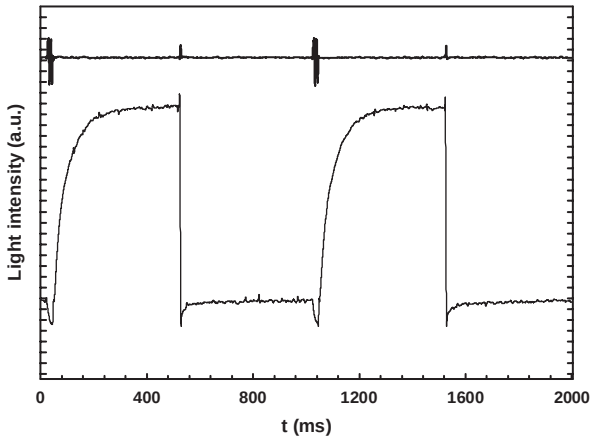

Fig. 4. Dynamic response based on our driving scheme with the slew-rate during the clearing time equal to about 0.175 V/μs. The drive voltage, clearing and writing frequencies are 37 V_{peak}, 100 Hz and 1 kHz respectively. It should compare with Fig. 5 in ref. 3. The small peak is the writing pulse whilst the large voltage swings are the clearing pulses.

3.2 *Dynamic response*

Due to the memory limitations in the waveform synthesis, the trapezoid waveform was implemented only during the clearing time. The slew-rate was about 0.175 V/μs and the frequency was 100 Hz. For consistency, we normalized the signal voltages relative to the drive voltage and the peak-to-peak value was quoted. We used 4ms writing time, 1 kHz data frequency, 0.64 focal-conic transition voltage and 0.14 data voltage which were the same as in our previous publication.[3] These were the parameters that gave rise to the good electro-optical characteristics. The dynamic response based on this scheme was shown in Fig. 4. Compared with the figure when the slew-rate was very fast (see Fig. 5 in ref. 3), the contrast and reflectance were not affected much, but the drive voltage had to increase from 34 V_{peak} to 37 V_{peak}.

In fact, if the slew-rate became lower than this value, the on-set of reflectance and contrast would shift to the high voltage side (Fig. 5). This was due to the constant energy requirement. The voltage dependence on the slew-rate is shown in Fig. 6(a). If the slew-rate is reduced, the peak voltage will have to increase to keep the energy constant. By comparing Fig. 2(b), Fig. 3(b) and Fig. 3(c) with Fig. 6(a), there will be an optimal S to obtain the best the electrical characteristics. In these cases, the rectangular voltage V_{P0} in eq. (5) is the lower bound drive voltage, which is determined by the

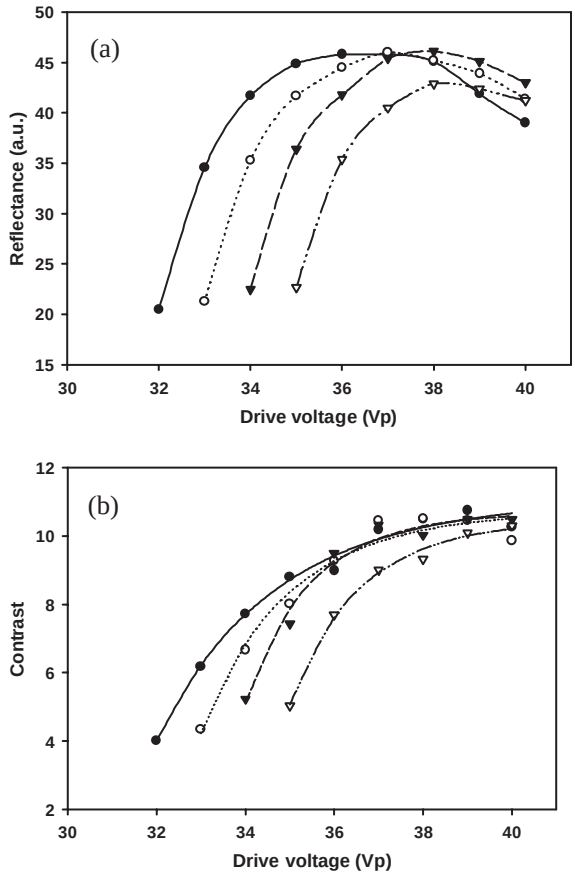

Fig. 5. (a) Reflectance and (b) contrast at different slew-rate: 79 V/ms (solid circle), 58 V/ms (hollow circle), 44 V/ms (solid triangle) and 35 V/ms (hollow triangle). Both are measured at the steady state and the waveform is trapezoid during the clearing time only. Other conditions are the same as in Fig. 4.

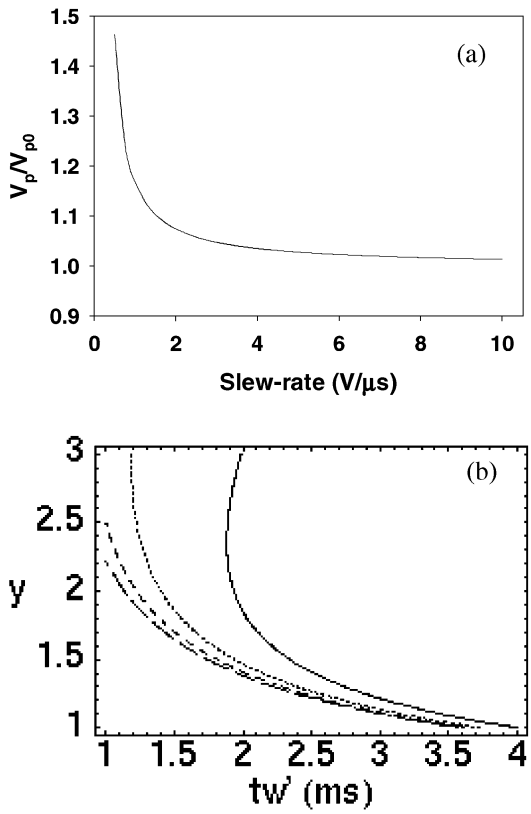

Fig. 6. (a) The voltage ratio against slew-rate and (b) increased voltage ratio against writing time t'_w at multiple slew-rates. For the latter case, all curves are referenced to the 4 ms/line addressing where $t_w = 4$ ms and $t_1 = 0.2$ ms. They are plotted at 4 times (long-dash), 3 times (dash), 2 times (dot) and 1 time (solid) the slew-rate equal to about 0.175 V/μs.

optimal electro-optic responses. Therefore, the break-even point of the slew-rate occurs at about 0.175 V/μs. This optimal slew-rate is obtained experimentally, and it is possible to deduce it by solving eq. (1), eq. (2) and eq. (5). In turn, it will set a constraint on the minimum addressing time per line or the maximum driving voltage.

To obtain the increase in the driving voltage, we chose the 4 ms/line addressing as the reference case. The results were shown in Fig. 6(b). It was noted that as the period t'_w was reduced below the total transition time $4t_1$, the waveform became triangular and its rms would be misleading on further increase in the voltage. We thus plotted the variation of voltage ratio as t'_w changed from 1 ms to 4 ms to ensure the proper scale and physical representation. The solid curve represents the voltage variation at the slew-rate equal to the reference (about 0.175 V/μs) and other curves are shown at the multiples of this value. If we relax the slew-rate to 0.35 V/μs (dot), the percentage increase for the 2 ms/line addressing compared with the 4 ms/line addressing at the reference slew-rate (solid) is about 50%, and i_{max} and $\langle p_{out} \rangle$ will become 2 mA/cm^2 and 3.6 mW/cm^2 respectively. Consequently, addressing at the 2 ms/line will add a higher cost compared with the 4 ms/line case. In addition, if it is to operate at the 1 ms/line addressing, the percentage increase will be double even the slew-rate is relaxed to 0.7 V/μs. Therefore, it will be very costly to operate the BCD with short and rapid pulses, since the maximum drive voltage and the power consumption are the key issues for portable applications.

4. Conclusions

Since the agreement between the experimental and the calculated results was good, we were able to justify the approximation and verified that the major conduction and power dissipation in the BCD depended mainly on the capacitance of the cholesteric liquid crystal. This was however not the case in nematic liquid crystal displays. The break-even point of the slew-rate for the optimal electrical and optical characteristics is about 0.175 V/μs. In this case, the maximum output current and average output power could be kept below 1 mA/cm^2 and 2 mW/cm^2 respectively. Therefore, for the most efficient VLSI implementation, 4 ms/line addressing would be the best choice. Combined with the demonstrated half voltage operation (less than 40 V_{pp}) in our previous studies, this already is comparable to the electrical requirements for the STN displays.[8,9]

Acknowledgment

This research was supported by the Hong Kong Government Industry Department.

1) Y. M. Zhu and D. K. Yang: SID '97 Dig. (1997) p. 97.
2) F. H. Yu and H. S. Kwok: SID '97 Dig. (1997) p. 659.
3) W. C. Yip and H. S. Kwok: Jpn. J. Appl. Phys. **39** (2000) 5169.
4) B. Taheri, J. W. Doane, D. Davis and D. St John: SID '96 Dig. (1996) p. 39.
5) W. D. St John, W. J. Fritz, Z. J. Lu and D. K. Yang: Phys. Rev. E **51** (1995) 1191.
6) A. Sugimura, N. Matsui, Y. Takahashi, H. Sonomura, H. Naito and M. Okuda: Phys. Rev. B **43** (1991) 8272.
7) A. Naito, M. Okuda and A. Sugimura: Phys. Rev. A **44** (1991) R3434.
8) T. Kurumisawa, A. Ito, S. Yamazaki and S. Iino: SID '96 Dig. (1996) p. 351.
9) M. Kitamura, A. Nakazawa, K. Kawaguchi, H. Motegi, Y. Hirai, T. Kuwata, H. Koh, M. Itoh and H. Araki: SID '96 Dig. (1996) p. 355.
10) A. Sugimura, Y. Takahashi and Z. Ou-Yang: Jpn. J. Appl. Phys. **32** (1993) 116.
11) P. G. de Gennes and J. Prost: *The Physics of Liquid Crystals* (Oxford University Press, New York, 1995).
12) T. Carlsson, F. M. Leslie and N. A. Clark: Phys. Rev. E **51** (1995) 4509.

Appendix

Since the display cell is modelled by simple circuit elements, the results in this section can be applied for the cholesteric and nematic liquid crystal displays. A good work which is different from the present discussion can be found in ref. 10. However, their results associated with the effective voltage on the liquid crystal layer should be taken with caution because the space charge equation should be in general a diffusion-type equation.[11] The coupling with the hydrodynamic equations cannot be neglected to account for the microscopic phenomena in the cholesteric liquid crystal displays.[12]

Now, by taking a Laplace transform, we have derived the current without making any approximation and assumption.

$$i(t) = SC_P(1 - \gamma(t)e^{-t/\tau}) \quad (0 \le t < 2t_1) \tag{A·1}$$

$$i(t) = SC_P(1 - \gamma(2t_1)e^{-2t_1/\tau})\frac{\cosh[\Omega(t - 2t_1) + \beta]}{\cosh\beta}e^{-(t-2t_1)/\tau} \quad \left(2t_1 \le t < \frac{T}{2}\right) \tag{A·2}$$

where the parametric functions are given by

$$\gamma(t) = \sqrt{1 - \lambda^2}\cosh(\Omega t + \alpha) + \frac{t_1}{\tau_1}\sqrt{1 - \mu^2}\cosh(\Omega t + \beta) \tag{A·3}$$

$$\alpha = \ln\left|\frac{1 + \lambda}{\sqrt{1 - \lambda^2}}\right| \tag{A·4}$$

$$\beta = \ln\left|\frac{1 + \mu}{\sqrt{1 - \mu^2}}\right| \tag{A·5}$$

$$\lambda = \frac{1}{\Omega}\left(\frac{1}{\tau} - \frac{1}{\tau_1}\right) \tag{A·6}$$

$$\mu = \frac{1}{\Omega}\left(\frac{1}{\tau} - \frac{1}{\tau_e}\right) \tag{A·7}$$

and the time constants are expressed as

$$\tau_1 = (R + R_P)C_P \tag{A·8}$$

$$\tau_2 = R_B C_B \tag{A·9}$$

$$\tau_e = (R + R_P)C \tag{A·10}$$

$$\tau = 2\left(\frac{\tau_2\tau_e}{\tau_2 + \tau_e}\right) \tag{A·11}$$

$$\Omega^2 = \frac{1}{\tau^2} - \frac{1}{\tau_1\tau_2} \tag{A·12}$$

Using eq. (A·8) to eq. (A·12), it is easy to show that λ^2 and μ^2 are both less than 1. In other words, eq. (A·1) to eq. (A·5) are well-defined equations. The definitions of the slew-rate S and the effective capacitance C can also be found in §2. It is noted that eq. (A·1) and eq. (A·2) are directly proportional to the capacitance of the polyimide layer C_P, and these findings are consistent with the literature.[10] It is however contrary to the dependence on the effective capacitance when the approximation is made [see §2]. Therefore, the approximation on the bulk resistance and the linear model are more appropriate to describe the experimental data.